IEEE Access
Multidisciplinary | Rapid Review | Open Access Journal

Date of publication xxxx 00, 0000, date of current version xxxx 00, 0000.

Digital Object Identifier 10.1109/ACCESS.2017.DOI

Enhanced Bioinspired Backstepping Control for a Mobile Robot with Unscented Kalman Filter

ZHE XU, SIMON X. YANG, (Senior Member, IEEE), and S. ANDREW GADSDEN, (Senior Member, IEEE)
School of Engineering, University of Guelph, Guelph, ON, N1G 2W1, CA

Corresponding author: Simon X. Yang (syang@uoguelph.ca).

This work is supported by the Advanced Robotic Intelligent Systems Laboratory at the University of Guelph under Natural Sciences and Engineering Research Council of Canada (NSERC)

ABSTRACT Tracking control has been an important research topic in robotics. It is critical to design controllers that make robotic systems with smooth velocity commands. In addition, the robustness of the robotic system in the presence of system and measurement noises is an important consideration as well. This paper presents a novel tracking control strategy that integrates a biologically inspired backstepping controller and a torque controller with unscented Kalman filter (UKF) and Kalman filter (KF). The bioinspired backstepping controller and torque controller are capable of avoiding and reducing the velocity jumps and overshoots that occur in conventional backstepping control and provide smooth velocity commands. The integration of KF and UKF enables the proposed control strategy capable of providing accurate state estimates. The stability and convergence of tracking errors are guaranteed by Lyapunov stability analysis. The novelty of the proposed bioinspired tracking control strategy is to take the system and measurement noises and robot dynamic constraints into the consideration. The results show that the proposed control strategy provides accurate state estimates and avoids large velocity jumps and overshoot that occurs in conventional backstepping control. This tracking control strategy is suitable for autonomous mobile robots under hard conditions with system and measurement noises.

INDEX TERMS Trajectory tracking, Bioinspired neural dynamics, Backstepping control, Torque control, Unscented Kalman filter

I. INTRODUCTION

Real-time tracking control has always been an essential research area in robotics [1], [2]. It is important to have the robotic system reach a certain speed that drives the robot to track its desired trajectory. In addition, accurately tracking the desired trajectory is an important task in real-life applications as well. The unmanned robotic systems usually operate in complex environments where the disturbances, especially the system and measurement noises, can affect the accuracy of the tracking. Therefore, it is necessary to make the robot accurately track its desired trajectory and robust to these noises. In addition, the tracking control method should be practically applicable for a mobile robot and easy to implement. The accuracy of control still remains a big challenge and many people are still doing research on it [3]–[5].

There have been many studies for tracking control of robots, and the research can be mainly divided into four different categories: 1) linearization [6]–[8]; 2) sliding mode [9]–[11]; 3) backstepping [12]–[16]; 4) neural networks and fuzzy systems [17]–[19]. All these methods have their pros and cons. The linearization method often uses state feedback linearization through a decoupling matrix, and this method requires small initial tracking error and suffers from large velocity changes in initial stages. The sliding mode control can deal with large initial tracking error, however, this control strategy usually suffers from a known chattering issue. The backstepping tracking method is the most commonly used method for tracking control. It deals with large initial tracking error, and the structure of this control method is relatively simple. The Lyapunov stability theory proves its stability. However, this approach generates velocity commands with large initial velocity jumps when tracking error

This article has been accepted for publication in a future issue of this journal, but has not been fully edited. Content may change prior to final publication. Citation information: DOI 10.1109/ACCESS.2020.3007881, IEEE Access

occurs, which makes this approach not practical. The neural network approach is an efficient way to deal with large velocity jump, however, this method requires online learning that is computationally complex, thus, this method is rather expensive to implement. The fuzzy rule method can also deal with velocity jumps, however, this rule-based approach is difficult to set up the rules, which are often based on general knowledge from human experience. Out of all these tracking control strategies, Yang *et al.* [14] proposed a novel backstepping controller that is inspired by a biological neural system. This method resolved velocity jumps in conventional backstepping control, and this biologically inspired backstepping control method is relatively simple to implement.

The KF is a well-known filter that provides optimal state estimates for linear systems under Gaussian noise. This filter has been widely used in many applications that include trajectory tracking [20]–[22]. Because the KF was designed for a linear system, multiple variations of KF have been developed to resolve the state estimation for nonlinear systems such as extended Kalman filter (EKF) [23] and UKF [24]. The UKF uses an unscented transform that is similar to a deterministic sampling technique. Unlike the commonly used EKF, the UKF does not require to linearize the system for this filter to operate.

The autonomous mobile robots usually operate under complex environment, which requires smooth velocity transitions for the robots. The complexity of the environment and noises may have huge impacts on the accuracy of the tracking for mobile robots. Therefore, this paper directly aims to tackle the problems that large velocity changes occurs in conventional backstepping control and robustness for accuracy trajectory tracking in noisy environment. The overall design should allow an autonomous mobile robot to operate smoothly with accurate state estimates in complex environments.

Many existing tracking methods assume the robot posture and velocity are known through real-time multi-sensor fusion, more specifically, the location and velocity of the robot are known through multiple sensor measurements, which are assumed to be completely accurate. In addition, the experiments are usually conducted in a laboratory environment, and does not consider the robot smooth speed transition. Therefore, the proposed control strategy focuses on resolving the noises that exist in real world situations for a mobile robot and providing smooth velocity transition. This paper developed a novel tracking control method that can generate smooth velocity commands and provide accurate state estimates by integrating the biologically inspired backstepping control and the torque control with KF and UKF. The main advantages of the proposed novel controller are summarized as follows:

1) In order to improve the accuracy of the trajectory tracking, the overall design considered both kinematics and dynamics of the mobile robot by integrating the biologically inspired backstepping controller with a torque controller for a mobile robot to further improve the tracking accuracy.

2) To further improve the accuracy of the trajectory tracking for real-life applications, the system and measurement noises are both taken into the consideration and therefore, the UKF and KF are respectively implemented to the kinematics and dynamic model of the mobile robot to provide accurate state estimates.

3) The overall novel tracking control provided a practical control strategy for a mobile robot operating under hard conditions. The proposed tracking control is capable of eliminating velocity jump issues and reducing the velocity overshoot issues in conventional backstepping control by the implementation of a bioinspired model. In addition, accurate state estimates are provided by the implementation of KF and UKF.

This paper is organized as follows, Section II provides the background of the different methods to be used in this paper. Then, Section III proposed the bioinspired backstepping and torque control with KF and UKF for the mobile robot. The simulation results are shown in Section IV with multiple comparisons to illustrate the improvement of the proposed control strategy. Finally, Section V provides the conclusion for the paper.

II. BACKGROUND

In this section, a dynamic and kinematic model of a nonholonomic robot are firstly presented. Then the KF and UKF algorithms and their applications to the mobile robot are introduced as well.

A. KINEMATICS AND DYNAMICS MODEL OF MOBILE ROBOT

Figure 1 demonstrates the model of a nonholonomic mobile robot in a 2D Cartesian workspace. The localization of the mobile robot is defined in the inertial frame as X, O, Y whereas the body-fixed frame is D, C, L, where D and L are the driving and lateral direction of the mobile robot, respectively, and C is the center point of the mobile robot. The posture of the nonholonomic robot in the inertial frame can be described as $P_c = [x_c, y_c, \theta_c]$, where x_c and y_c denotes the spacial position at point C of mobile robot and θ_c is the orientation angle with respect to point C. The mobile robot is subjected to a nonholonomic kinematic constraint which is given as

$$\dot{y}_c \cos\theta_c - \dot{x}_c \sin\theta_c = 0 \tag{1}$$

This nonholonomic constraint makes the robot move normal to the driving wheels. From the perspective of kinematic control, without considering the slipping condition the mobile robot has 2 degrees of freedom (DOF). The relationship between the velocity of the mobile robot in the inertial frame, $\dot{P}_c = [\dot{x}_c, \dot{y}_c, \dot{\theta}_c]$, and velocity of the mobile robot in the body-fixed frame is obtained through a Jacobian matrix as

$$\dot{P}_c = \begin{bmatrix} \dot{x}_c \\ \dot{y}_c \\ \dot{\theta}_c \end{bmatrix} = \begin{bmatrix} \cos\theta_c & 0 \\ \sin\theta_c & 0 \\ 0 & 1 \end{bmatrix} \begin{bmatrix} \upsilon_c \\ \omega_c \end{bmatrix} \tag{2}$$

This article has been accepted for publication in a future issue of this journal, but has not been fully edited. Content may change prior to final publication. Citation information: DOI 10.1109/ACCESS.2020.3007881, IEEE Access

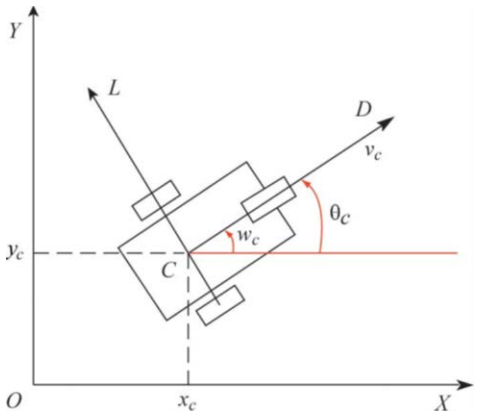

FIGURE 1: Model of a nonholonomic mobile robot.

where υ_c and ω_c represent the linear and angular velocity of the mobile robot in the body-fixed frame, respectively. The equation of motion for the nonholonomic mobile robot without considering the effect of gravity can be described as follows

$$\bar{M}(P_c)\dot{V} + \bar{F}(P_c,\dot{P}_c)V + \bar{\tau}_d = \bar{B}\tau_c \tag{3}$$

where $\bar{M}(P_c)$ is the positive definite matrix for inertia, and $\bar{F}(P_c,\dot{P})$ is the centripetal and Coriolis matrix, $\bar{\tau}_d$ is the disturbances, and $V = [\upsilon_c, \omega_c]^{\mathrm{T}}$

$$\begin{aligned} \bar{M} &= \begin{bmatrix} m & 0 \\ 0 & I \end{bmatrix} \bar{F} = \begin{bmatrix} 0 & 0 \\ 0 & 0 \end{bmatrix} \\ \bar{B} &= \frac{1}{r}\begin{bmatrix} 1 & 1 \\ l & l \end{bmatrix} \tau_c = \begin{bmatrix} \tau_R \\ \tau_L \end{bmatrix} \end{aligned} \tag{4}$$

where m is the mass of the mobile robot, I is the inertia of the mobile robot, and τ_R and τ_L are the right and left wheel torque inputs that are generated from the DC motors, respectively. Parameter r is the radius of the driving wheels and l is the azimuth length from point C to the driving wheels. By considering $\bar{\tau}_d$ as external disturbance, the simplified dynamics of the mobile robot is expressed as

$$\dot{V} = \bar{M}^{-1}\bar{B} \cdot \tau_c \tag{5}$$

B. ERROR DYNAMICS

The desired posture of the mobile robot, $P_d(t) = [x_d(t), y_d(t), \theta_d(t)]^{\mathrm{T}}$, is obtained through its reference path from the inertial frame. Defining the tracking error of the mobile robot in the body-fixed frame as $e_P(t) = [e_D(t), e_L(t), e_\theta(t)]^{\mathrm{T}}$, where e_D, e_L, and e_θ are the tracking errors in the driving direction, lateral direction, and orientation, respectively. The tracking errors of the mobile robot from the inertial frame to the body-fixed is calculated through a transformation matrix T_e by

$$e_P = \begin{bmatrix} e_D \\ e_L \\ e_\theta \end{bmatrix} = \begin{bmatrix} \cos\theta_c & \sin\theta_c & 0 \\ -\sin\theta_c & \cos\theta_c & 0 \\ 0 & 0 & 1 \end{bmatrix} \begin{bmatrix} e_x \\ e_y \\ e_\theta \end{bmatrix} \tag{6}$$

where $e_x = x_d - x_c$, $e_y = y_d - y_c$, and $e_\theta = \theta_d - \theta_c$ denote the tracking error in X, Y, and orientation θ in the inertia frame, respectively.

The error dynamics can be derived from (6) by taking its time derivative as

$$\begin{bmatrix} \dot{e}_D \\ \dot{e}_L \\ \dot{e}_\theta \end{bmatrix} = \begin{bmatrix} \omega_c e_L - \upsilon_c + \upsilon_d \cos e_\theta \\ -\omega_c e_D + \upsilon_d \sin e_\theta \\ \omega_d - \omega_c \end{bmatrix} \tag{7}$$

where υ_d and ω_d represent the linear and angular velocity of the mobile robot, respectively. Given the desired posture P_d, of the mobile robot, υ_d and ω_d are calculated by

$$\upsilon_d = \sqrt{{x_d}^2 + {y_d}^2} \tag{8}$$

$$\omega_d = \frac{\ddot{y}_d\dot{x}_d - \ddot{x}_d\dot{y}_d}{\dot{x}_d^2 + \dot{y}_d^2} \tag{9}$$

C. KF AND UKF ALGORITHMS

Given a linear system with noises as

$$x_{k+1} = Ax_k + Bu_k + \alpha_k \tag{10}$$

$$z_{k+1} = Hx_{k+1} + \beta_{k+1} \tag{11}$$

where A is the system matrix and B is the input matrix, u_k is the input, and H is the measurement matrix. Both system and measurement noises are treated as Gaussian, where $P(\alpha_k) \sim N(0, Q_k)$, and $P(\beta_k) \sim N(0, R_k)$. Both noises are determined by the actual experiments and have effects on the actual state value x_k and its measurement value z_k. Then, the processes of the KF can be defined in the following five procedures as

$$\hat{x}_{k+1|k} = A\hat{x}_{k|k} + Bu_k \tag{12}$$

$$P_{k+1|k} = AP_{k|k}A^T + Q_k \tag{13}$$

where $\hat{x}_{k+1|k}$ and $\hat{x}_{k|k}$ are the priori and posterior state estimates, respectively, and $P_{k+1|k}$ is the corresponding state error matrix, which is the covariance of the process noise, Q_k is the system noise covariance. Following the predicting stage from (12) and (13), the updating stage is defined as

$$K_{k+1} = P_{k+1|k}H^T[HP_{k+1|k}H^T + R_{k+1}]^{-1} \tag{14}$$

$$\hat{x}_{k+1|k+1} = \hat{x}_{k+1|k} + K_{k+1}[z_{k+1} - H\hat{x}_{k+1|k}] \tag{15}$$

$$P_{k+1|k+1} = [I - K_{k+1}H]P_{k+1|k} \tag{16}$$

where Kalman gain K_{k+1} is used in minimizing the trace of the posteriori state error covariance matrix, $\hat{x}_{k+1|k+1}$ is the updated state estimate, $P_{k+1|k+1}$ is the posteriori state error covariance, and R_k is the measurement noise covariance.

In real world applications, there is no perfect linear system and therefore a variation of KF, which is called UKF, has been developed to deal with nonlinear systems. The general form of a nonlinear system and its measurement model can be defined as

$$x_{k+1} = f(x_k, u_k) + \delta_k \tag{17}$$

This article has been accepted for publication in a future issue of this journal, but has not been fully edited. Content may change prior to final publication. Citation information: DOI 10.1109/ACCESS.2020.3007881, IEEE Access

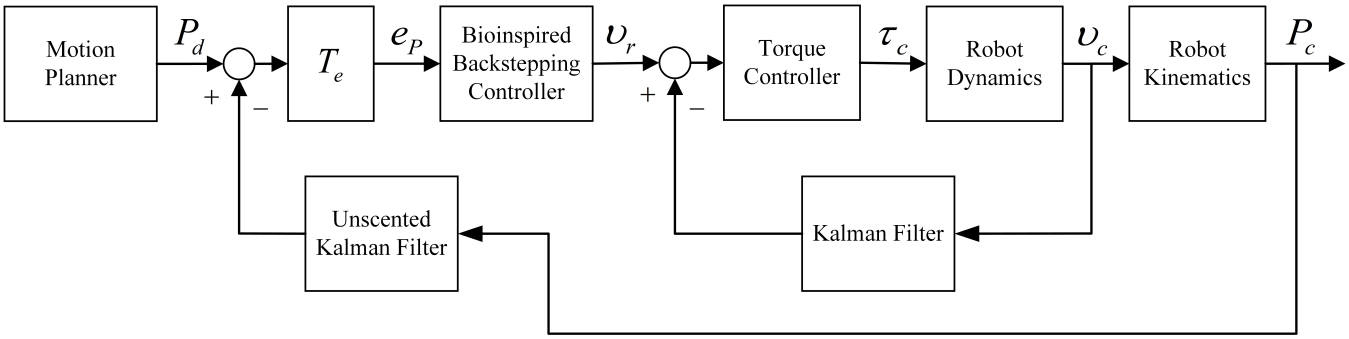

FIGURE 2: The block diagram of the proposed tracking control with KF and UKF.

$$z_{k+1} = h(x_{k+1}) + \gamma_{k+1} \tag{18}$$

where $f(x_k, u_k)$ is the nonlinear process of the system and h is the measurement model of the system, δ_k and γ_k are the Gaussian process and measurement noises, respectively. The first process of the UKF is to generate $2n+1$ sampling points, which are called sigma points, and n is the dimension of the state variable x_k. The state estimate of the mobile robot is then generated by these sigma points through weighting and multiple nonlinear functions. The initial sigma point, $x_{0,k|k}$ and its weight, W_0, are calculated by

$$x_{0,k|k} = \hat{x}_{k|k} \tag{19}$$

$$W_0 = \frac{\lambda}{n+\lambda} \tag{20}$$

where λ is a design value that controls the spread of sigma points and it is usually set significantly less than 1. Then the second to $(n+1)$-th point are defined as

$$X_{i,k|k} = \hat{x}_{k|k} + (\sqrt{(n+\lambda)P_{k|k}})_i \tag{21}$$

$$W_i = \frac{1}{[2(n+\lambda)]} \tag{22}$$

where $X_{i,k|k}$ and W_i are the corresponding sigma point and weight for i-th sigma point. The final n sigma points are defined as

$$X_{i+n,k|k} = \hat{x}_{k|k} - (\sqrt{(n+\lambda)P_{k|k}})_i \tag{23}$$

$$W_{i+n} = \frac{1}{[2(n+\lambda)]} \tag{24}$$

From (19) to (24), the predicted state estimate, $\hat{x}_{i,k+1|k}$ is calculated by

$$\hat{X}_{i,k+1|k} = f(\hat{X}_{i,k|k}, u_k) \tag{25}$$

$$\hat{x}_{i,k+1|k} = \sum_{i=0}^{2n} W_i \hat{X}_{i,k+1|k} \tag{26}$$

and predicted state error covariance $P_{k+1|k}$ is obtained through

$$P_{k+1|k} = \sum_{i=0}^{2n} W_i (\hat{X}_{i,k+1|k} - \hat{x}_{k+1|k})(\hat{X}_{i,k+1|k} - \hat{x}_{k+1|k})^{\mathrm{T}} + Q_k \tag{27}$$

All the generated samples are then used to obtain the predicted measurement by nonlinear measurement model, the predicted measurement is defined as

$$\hat{Z}_{i,k+1|k} = h(\hat{X}_{i,k+1}, u_k) \tag{28}$$

$$\hat{z}_{k+1|k} = \sum_{i=0}^{2n} W_i \hat{Z}_{i,k+1|k} \tag{29}$$

where $\hat{Z}_{i,k+1|k}$ is the i-th measurement and $\hat{z}_{k+1|k}$ is the predicted measurement. Then, these two variables are used to calculate the measurement covariance $P_{zz,k+1|k}$ and cross-covariance $P_{xz,k+1|k}$, which are defined as

$$P_{zz,k+1|k} = \sum_{i=0}^{2n} W_i (\hat{Z}_{i,k+1|k} - \hat{z}_{k+1|k})(\hat{Z}_{i,k+1|k} - \hat{z}_{k+1|k})^{\mathrm{T}} + R_k \tag{30}$$

$$P_{xz,k+1|k} = \sum_{i=0}^{2n} W_i (\hat{X}_{i,k+1|k} - \hat{x}_{k+1|k})(\hat{Z}_{i,k+1|k} - \hat{z}_{k+1|k})^{\mathrm{T}} \tag{31}$$

Finally, the Kalman gain, state estimate, and state error covariance are respectively obtained through

$$K_{k+1} = P_{xz,k+1|k} P_{zz,k+1|k}^{-1} \tag{32}$$

$$\hat{x}_{k+1|k+1} = \hat{x}_{k+1|k} + K_{k+1}(z_{k+1} - \hat{z}_{k+1|k}) \tag{33}$$

$$P_{k+1|k+1} = P_{k+1|k} - K_{k+1} P_{zz,k+1|k} K_{k+1}^{\mathrm{T}} \tag{34}$$

The UKF provides accurate state estimates for the nonlinear system with noises. Although there are many other nonlinear filters such as EKF, the reason why this paper chooses to implement the UKF is that this method does not require linearization compared to EKF.

D. THE KF AND UKF MODEL FOR THE MOBILE ROBOT

Based on (3)-(5), knowing the time step Δt, using Euler approximation, the KF state model for the dynamics of the mobile robot is defined as

$$\hat{V}_{k+1}^{-} = \begin{bmatrix} \hat{v}_{c,k+1}^{-} \\ \hat{\omega}_{c,k+1}^{-} \end{bmatrix} = \begin{bmatrix} \hat{v}_{c,k} \\ \hat{\omega}_{c,k} \end{bmatrix} + \bar{M}^{-1} \bar{B} \tau_{c,k} \cdot \Delta t + \alpha_k \tag{35}$$

This article has been accepted for publication in a future issue of this journal, but has not been fully edited. Content may change prior to final publication. Citation information: DOI 10.1109/ACCESS.2020.3007881, IEEE Access

where $\hat{v}_{c,k}$ and $\hat{\omega}_{c,k}$ are respectively the estimated linear and angular velocity at time k, $\hat{v}^-_{c,k+1}$ and $\hat{\omega}^-_{c,k+1}$ are respectively the priori estimates of the linear and angular velocity at time $k+1$, α_k is the system noise for the mobile robot. The measurement for the dynamics of the mobile robot is calculated by

$$\tilde{V}_{k+1} = H(\hat{V}^-_{k+1}, \beta_{k+1}) = H \begin{bmatrix} \hat{v}^-_{c,k+1} \\ \hat{\omega}^-_{c,k+1} \end{bmatrix} + \beta_{k+1} \quad (36)$$

where $\tilde{V}_{k+1}$ and β_{k+1} are the measured velocity vector and the measurement noise at time $k+1$, respectively. The system and measurement noises are presented in the mobile robot due to the sophisticated design of the mobile robot.

As for the UKF, the state and measurement model for the kinematics of the mobile robot is treated as

$$\hat{P}^-_{c,k+1} = \begin{bmatrix} \hat{x}^-_{c,k+1} \\ \hat{y}^-_{c,k+1} \\ \hat{\theta}^-_{c,k+1} \end{bmatrix} = \begin{bmatrix} \hat{x}_{c,k} + \cos\hat{\theta}_{c,k}\hat{v}_{c,k}\Delta t \\ \hat{y}_{c,k} + \sin\hat{\theta}_{c,k}\hat{v}_{c,k}\Delta t \\ \hat{\theta}_{c,k} + \hat{\omega}_{c,k}\Delta t \end{bmatrix} + \delta_k \quad (37)$$

$$\tilde{P}_{c,k+1} = h(\hat{P}^-_{c,k+1}, \gamma_{k+1}) = h \begin{bmatrix} \hat{x}^-_{c,k+1} \\ \hat{y}^-_{c,k+1} \\ \hat{\theta}^-_{c,k+1} \end{bmatrix} + \gamma_{k+1} \quad (38)$$

where $\hat{x}_{c,k}$, $\hat{y}_{c,k}$, and $\hat{\theta}_{c,k}$ are the estimates of the robot positions at time k, $\hat{x}^-_{c,k+1}$, $\hat{y}^-_{c,k+1}$, and $\hat{\theta}^-_{c,k+1}$ are the priori estimates of the robot position at time $k+1$. The process noise is added by using dead reckoning the location $P^-_{c,k+1}$. In addition, the kinematic model has measurement noises γ_k. The UKF is used to provide accurate state estimates. The UKF uses the unscented transform technique, there are 7 sigma points being generated since states x_c, y_c, and θ_c are being considered in the kinematic model of the mobile robot. In addition, the system and measurement noises are both considered as zero mean Gaussian noises.

III. DESIGN OF CONTROLLERS

This section designs a kinematic controller and a dynamic controller that integrate with KF and UKF. The proposed enhanced controller not only solves the speed jump issue that occurs in the conventional backstepping control but also provides accurate state estimates overall. The total design of this novel tracking controller is presented in Figure 2. The entire system has two closed-loops, which contain bioinspired control and torque control. The feedbacks for torque control and bioinspired backstepping control are respectively propagated through KF and UKF to generate accurate state estimates for the better performance of the control strategy in order for a mobile robot operating in hard conditions.

A. BIOINSPIRED BACKSTEPPING CONTROLLER

The conventional backstepping tracking control law for a nonholonomic mobile robot is provided as [25]

$$v_r = C_1 e_D + v_d \cos e_\theta \quad (39)$$

$$\omega_r = \omega_d + C_2 v_d e_L + C_3 v_d \sin e_\theta \quad (40)$$

where C_1, C_2, and C_3 are the designed parameters, v_r and ω_r are respectively the reference linear and angular velocity command that generated from the controller. This control law has a speed jump issue. Therefore, Yang *et al.* [14] proposed a bioinspired backstepping control that used the dynamics of voltage across the membrane, which is called the shunting model. This model is written as

$$C_m \frac{dV_m}{dt} = -(E_p + V_m)g_p + (E_{Na} - V_m)g_{Na} - (E_k + V_m)g_K \quad (41)$$

where C_m is the membrane capacitance, Parameter E_p, E_{Na}, and E_k are the Nernst potentials for the passive leak, sodium ions, and potassium ions in the membrane, respectively. Parameter g_p, g_{Na}, and g_K denote the conductance of the passive channel, sodium, and potassium, respectively. This model is the foundation of the shunting model, which leads to many variations and applications.

By setting $C_m = 1$ and substituting $x_i = E_p + V_m$, $A_1 = g_p$, $B_1 = E_{Na} + E_p$, $D_1 = E_k - E_p$, $S_i{}^+ = g_{Na}$, and $S_i{}^- = g_K$ into (41), the shunting model can be rewritten as

$$\frac{dx_i}{dt} = -A_1 x_i + (B_1 - x_i)S_i{}^+ - (D_1 + x_i)S_i{}^- \quad (42)$$

where x_i is the neural activity of the i-th neuron. Parameters A_1, B_1, and D_1 are nonnegative constants that represent passive decay rate and the upper and lower bounds of the neural activity, respectively. Variable $S_i{}^+$ and $S_i{}^-$ denote the excitatory and inhibitory inputs to the neuron. This model was first used in real-time path planning for robots by Yang and Meng [26]. The conventional backstepping control has speed jump and overshoot issues, some recent research used backstepping technique with the combination of sliding mode control, however, the overshoot and jump issue can still be observed [27]–[29], and the speed jump issue has not been practically solved. The proposed tracking control strategy is able to eliminate the velocity jump and overshoot that occur in conventional backstepping control and provide smooth velocity commands.

With the implementation of the shunting model into conventional backstepping control, the bioinspired backstepping control laws are defined as

$$v_r = v_s + v_d \cos e_\theta \quad (43)$$

$$\omega_r = \omega_d + C_2 v_d e_L + C_3 v_d \sin e_\theta \quad (44)$$

where v_s is from a neural dynamics equation with respect to the error in the driving direction as

$$\frac{dv_s}{dt} = -A_1 v_s + (B_1 - v_s)f(e_D) - (D_1 + v_s)g(e_D) \quad (45)$$

where $f(e_D) = \max\{e_D, 0\}$ is the linear above threshold function and $g(e_D) = \max\{-e_D, 0\}$ is a nonlinear function. Parameter A_1 is the passive decay rate, and B_1 and D_1 are upper and lower bound of the velocity, respectively.

This article has been accepted for publication in a future issue of this journal, but has not been fully edited. Content may change prior to final publication. Citation information: DOI 10.1109/ACCESS.2020.3007881, IEEE Access

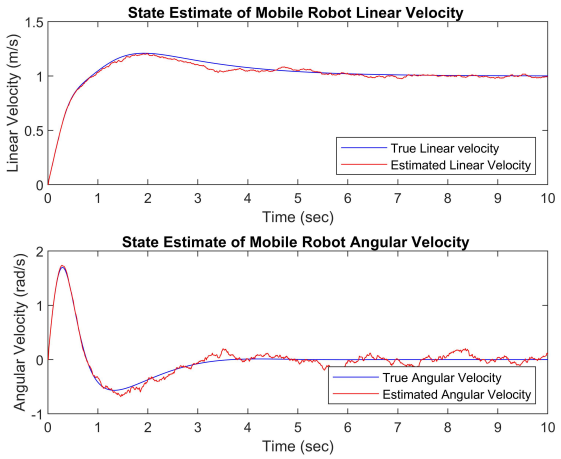

FIGURE 3: Velocities estimates for straight line tracking.

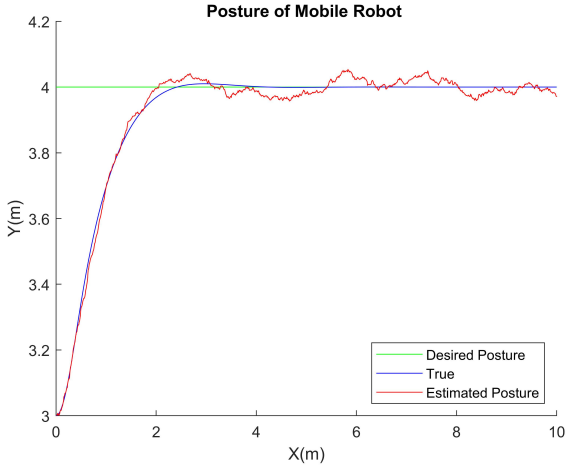

FIGURE 4: Posture of mobile robot for straight line tracking.

The Lyapunov candidate function and its time derivative for bioinspired backstepping control are proposed as

$$V_1 = \frac{1}{2}{e_D}^2 + \frac{1}{2}{e_L}^2 + \frac{1}{C_2}(1-\cos e_\theta) + \frac{1}{2B_1}{v_s}^2 \quad (46)$$

$$\dot{V}_1 = \dot{e}_D e_D + \dot{e}_L e_L + \frac{1}{C_2}\dot{e}_\theta \sin e_\theta + \frac{1}{B_1}\dot{v}_s v_s \quad (47)$$

B. TORQUE CONTROLLER

The actual velocity of the mobile robot is different from the velocity command that is generated from the bioinspired backstepping control due to the noises. The velocity tracking error e_η is expressed as

$$e_\eta = \begin{bmatrix} e_v \\ e_\omega \end{bmatrix} = \begin{bmatrix} v_r - v_c \\ \omega_r - \omega_c \end{bmatrix} \quad (48)$$

Then the torque tracking control law $\tau_c = [\tau_L, \tau_R]^{\mathrm{T}}$ is proposed as

$$\tau_L = \frac{mr}{2}(\dot{v}_r + C_4 e_v) - \frac{Ir}{2c}(\dot{\omega}_r + C_5 e_\omega) \quad (49)$$

$$\tau_R = \frac{mr}{2}(\dot{v}_r + C_4 e_v) + \frac{Ir}{2c}(\dot{\omega}_r + C_5 e_\omega) \quad (50)$$

The Lyapunov candidate function and its time derivative for the torque controller can be defined as

$$V_2 = V_1 + \frac{1}{2}{e_v}^2 + \frac{1}{2}{e_\omega}^2 \quad (51)$$

$$\dot{V}_2 = \dot{V}_1 + e_v\dot{e}_v + e_\omega\dot{e}_\omega = \dot{V}_1 + e_v(\dot{v}_r - \dot{v}_c) + e_\omega(\dot{\omega}_r - \dot{\omega}_c) \quad (52)$$

C. STABILITY ANALYSIS

To prove the stability of the proposed control strategy, the bioinspired backstepping controller and torque controller are firstly proven to be asymptotically stable. The overall stability is then proven as well. It is assumed that the posture

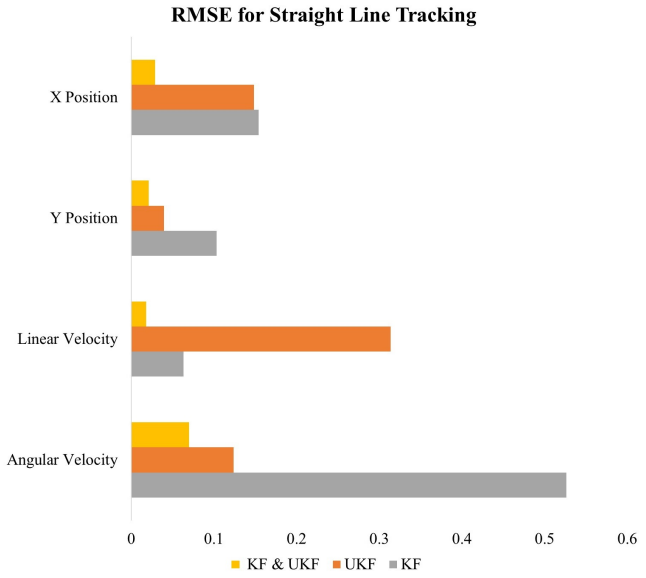

FIGURE 5: RMSE for straight line tracking.

and velocity errors are bounded. First, based on (43)-(45) and (47), $\dot{V}_1$ is rewritten as

$$\dot{V}_1 = -v_s e_D - \frac{C_3}{C_2}v_d \sin^2 e_\theta + \frac{1}{B_1}[-A_1 - f(e_D) - g(e_D)]{v_s}^2 + \frac{1}{B_1}[B_1 f(e_D) - D_1 g(e_D)]v_s \quad (53)$$

Assuming $B_1 = D_1$, (53) is rewritten as

$$\dot{V}_1 = -\frac{C_3}{C_2}v_d \sin^2 e_\theta + \frac{1}{B_1}[-A_1 - f(e_D) - g(e_D)]{v_s}^2 + [f(e_D) - g(e_D) - e_D]v_s \quad (54)$$

Based on the definition of $f(e_D)$ and $g(e_D)$. If $e_D \geq 0$, $f(e_D) = e_D$ and $g(e_D) = 0$, then

$$[f(e_D) - g(e_D) - e_D]v_s = e_D - 0 - e_D = 0 \quad (55)$$

This article has been accepted for publication in a future issue of this journal, but has not been fully edited. Content may change prior to final publication. Citation information: DOI 10.1109/ACCESS.2020.3007881, IEEE Access

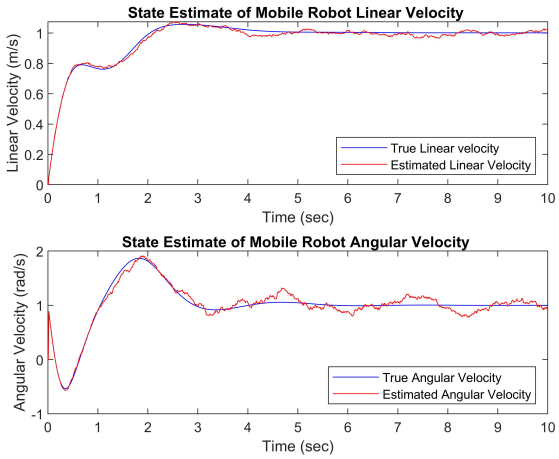

FIGURE 6: Velocities estimates for circular line tracking.

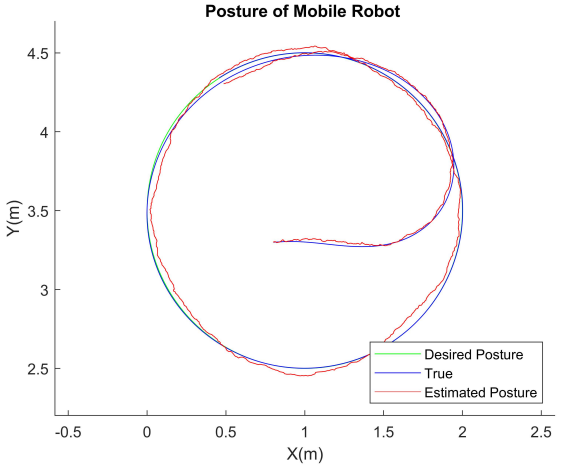

FIGURE 7: Posture of mobile robot for circular line tracking.

By applying the same concept from (55), if $e_D \leq 0$, $g(e_D) = e_D$ and $f(e_D) = 0$, then

$$[f(e_D) - g(e_D) - e_D]v_s = 0 - (-e_D) - e_D = 0 \quad (56)$$

Therefore, (54) becomes

$$\dot{V}_1 = -\frac{C_3}{C_2} v_d \sin^2 e_\theta + \frac{1}{B_1}[-A_1 - f(e_D) - g(e_D)]{v_s}^2 \quad (57)$$

The C_3 and C_2, and v_d are positive constants. $g(e_D)$ and $f(e_D)$ are nonnegative, and A_1 and B_1 are nonnegative constants. Therefore, $\dot{V}_1 \leq 0$. If and only if $e_D = 0$ and $e_\theta = 0$, then $\dot{V}_1 = 0$, thus the torque controller is asymptotically stable.

To prove the stability of the torque controller, by applying (5) into (52), the equation becomes

$$\dot{V}_2 = \dot{V}_1 + e_v(\dot{v}_r - \frac{1}{mr}\tau_L - \frac{1}{mr}\tau_R) + e_\omega(\dot{\omega}_r + \frac{l}{Ir}\tau_L - \frac{l}{Ir}\tau_R) \quad (58)$$

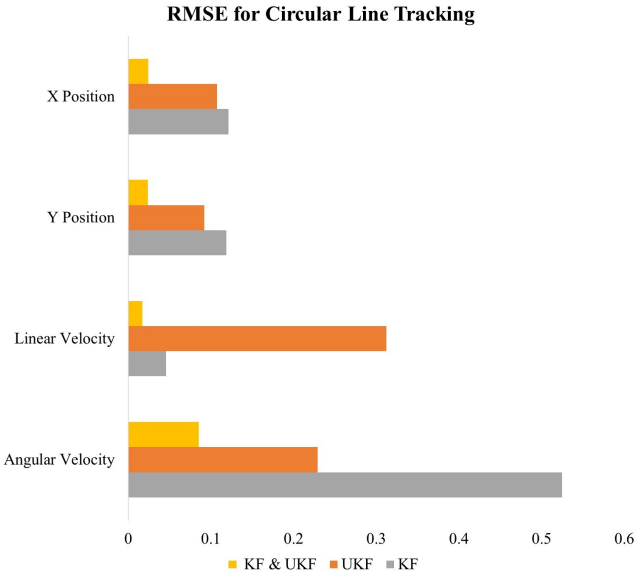

FIGURE 8: RMSE for circular line tracking.

by replacing τ_L and τ_R in (49) and (50) in (58), the $\dot{V}_2$ is rewritten as

$$\dot{V}_2 = \dot{V}_1 - C_4{e_v}^2 - C_5{e_\omega}^2 \quad (59)$$

Since $\dot{V}_1$, $-C_4{e_v}^2$, and $-C_5{e_\omega}^2$ are all less than or equal to zero, the proposed torque controller reaches a stable condition. If and only if e_D, e_θ, and e_η are zeros, then $\dot{V}_2 = 0$, therefore, the torque control is asymptotically stable. For the overall stability analysis, the Lyapunov candidate function of the system can be defined as

$$V_3 = V_1 + V_2 \quad (60)$$

The time derivative of V_3 is derived as

$$\dot{V}_3 = 2(-\frac{C_3}{C_2} v_d \sin^2 e_\theta + \frac{1}{B_1}[-A_1 - f(e_D) - g(e_D)]v_s) - C_4{e_v}^2 - C_5{e_\omega}^2 \quad (61)$$

If and only if the e_P and e_η are zeros, $\dot{V}_3 = 0$. Therefore, when $e_\theta = [-\pi, \pi]$, the control system is globally asymptotically stable.

IV. RESULTS

In this section, the proposed tracking control that integrated with KF and UKF are used to track a straight line and a curved line. The results show that the proposed control strategy with KF and UKF track the desired trajectory with smooth velocity command and the KF and UKF provide accurate state estimates. The designed control value λ is set as e^{-3} as it is the most suitable value for Gaussian [30]. The initial state error covariance for dynamic model $P_{(0|0)} = 10Q$, system noise covariance Q, and measurement noise covariance R for linear and angular velocity are treated as $Q = \text{diag}(e^{-5}, e^{-6})$, and $R = \text{diag}(e^{-2}, e^{-3})$. The process

This article has been accepted for publication in a future issue of this journal, but has not been fully edited. Content may change prior to final publication. Citation information: DOI 10.1109/ACCESS.2020.3007881, IEEE Access

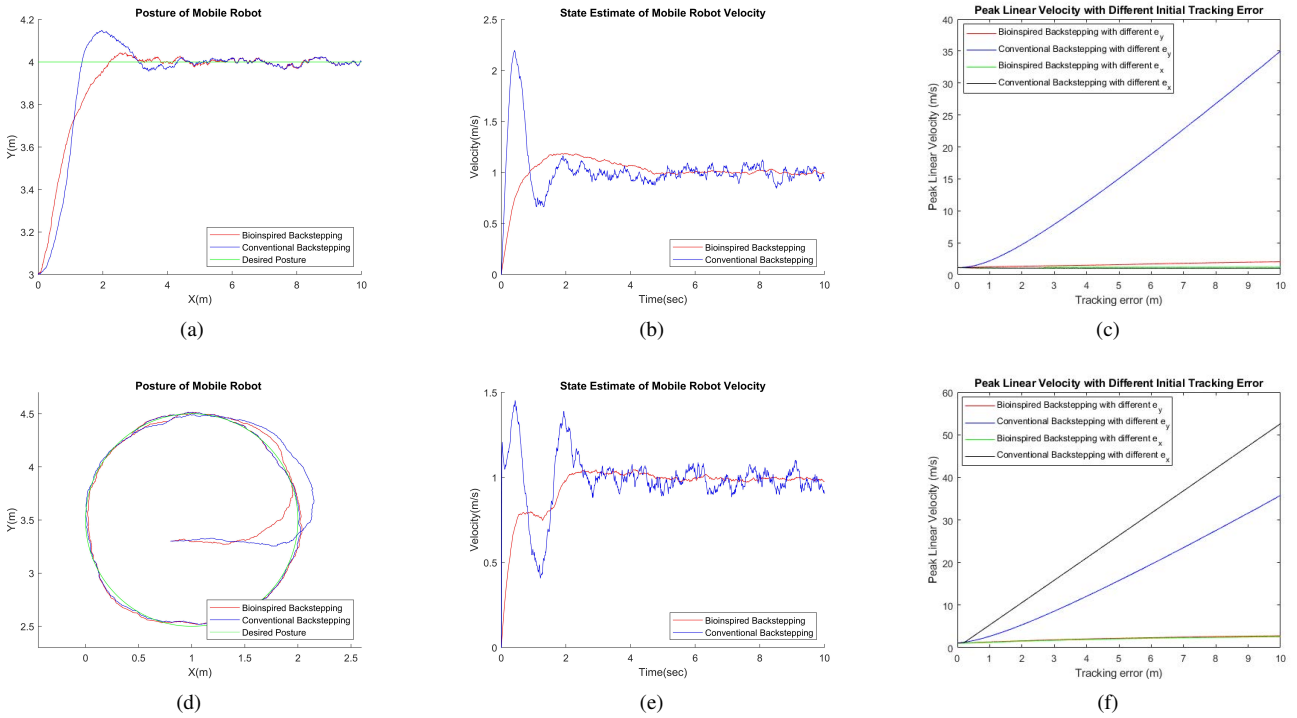

FIGURE 9: Robot posture, velocity, and peak velocity comparisons between conventional and bioinspired backstepping control: (a) Straight path tracking performance; (b) Straight path tracking linear velocity estimates; (c) Peak linear velocity comparison for straight path tracking; (d) Circular path tracking performance; (e) Circular path tracking linear velocity estimates; (f) Peak linear velocity comparison for circular path tracking.

noise covariance of mobile robot using dead reckoning is given as diag(e^{-5}, e^{-5}, e^{-6}) and measurement noise covariance for the posture of mobile robot is diag(e^{-2}, e^{-2}, e^{-3}). The measurement model H for KF and h for UKF are treated as 2×2 and 3×3 identity matrices, respectively [31], [32]. To validate the efficiency of the KF and UKF in the proposed control strategy, the root mean square error (RMSE) is used to calculate the error between the actual mobile robot path and the path without noises being present in the mobile robot. The mobile robot parameters are set as $m = 10$, $I = 0.1$, $l = 1$, and $r = 1$. The RMSE is calculated by

$$\text{RMSE} = \sqrt{\sum_{i=1}^{N} \frac{\left(P - \tilde{P}\right)^2}{N}} \tag{62}$$

where P is the mobile robot state without noise being presented and $\tilde{P}$ is the estimated state of the mobile robot, and N is the total amount of samples that are collected.

To further evaluate the smoothness of the proposed tracking method, the linear and angular acceleration of the mobile robot are calculated to show that the proposed tracking method is capable of providing smooth velocity command for a mobile robot.

A. TRACKING A STRAIGHT PATH

To show that the proposed control strategy is capable of tracking the desired trajectory, the desired path is defined as $y = 4$ and $x = 0$. In a 2D Cartesian workspace, the posture of the initial position of the mobile robot is defined as $(0, 3)$. Therefore, the initial tracking error is $(0, 1)$. The sampling frequency is set to be 100Hz. The parameters for the bioinspired backstepping controller are chosen as $C_2 = 5$ and $C_3 = 2$, $A_1 = 5$, $B_1 = 3$, and $D_1 = 3$. The parameters for the torque controller are set as $C_4 = 5$ and $C_5 = 5$. From Figure 3 and Figure 4, it is obvious that the tracking control with KF and UKF provides more accurate state estimates compared to the method without filters. Figure 5 provides a better view of the results, which shows the proposed method provides more accurate state estimates over any single implementation of the filters. Without the implementation of the filters the average tracking error reaches 1.8215m, which makes the measured data unusable. In addition, the combination of bioinspired controller and torque controller is able to reduce the tracking error. The average tracking error without torque controller being presented is 0.0438m, with the implementation of torque controller, the average tracking error has been reduced to 0.0275m.

B. TRACKING A CIRCULAR PATH

A circular path is defined to show that the proposed tracking strategy is capable of tracking a curved path. The initial desired posture of the mobile robot is at (1, 2.5), whereas the actual robot posture is at (0.8, 3.3). The parameters are chosen as $C_2 = 5$ and $C_3 = 2$, $A_1 = 5$, $B_1 = 3$, and $D_1 = 3$ for the bioinspired backstepping controller. The parameters for the torque controller are set as $C_4 = 5$ and $C_5 = 5$. The sampling frequency is 100Hz. The results in Figure 7 shows that the robot tracks the desired path accurately. In addition, Figure 6 shows that the estimated velocity is smoother with the application of the KF and UKF, thus the results are more promising. In order to show that the proposed controller performed better with the filter for a circular path, the RMSE in Figure 8 addresses the efficiency with each method, without the implementation of the filters, the average position tracking error reaches 1.6368m. The average position tracking error for bioinspired backstepping and torque control is 0.0269m in comparison to 0.0545m with only bioinspired backstepping control being implemented.

C. TRACKING SMOOTHNESS

For a mobile robot operating under hard conditions, the smoothness of the path and velocities are essential to ensure the robots functionality. Therefore, the comparison study between conventional backstepping and bioinspired backstepping control with filters is performed. The parameters for the conventional backstepping control are set as $C_1 = 5$, $C_2 = 5$, and $C_3 = 2$, and the parameters for the bioinspired backstepping control are set as $C_2 = 5$, $C_3 = 2$, $A_1 = 5$, $B_1 = 3$, and $D_1 = 3$.

As shown in Figure 9(a), the robot path to track a straight line for the bioinspired tracking control is smoother than the conventional backstepping control. In addition, Figure 9(b) shows that the generated linear velocity for the bioinspired tracking method is smoother than the conventional backstepping control tracking method as well. In addition, the peak linear velocity of mobile robot that is required for the bioinspired tracking method is much lower than the conventional backstepping control. The maximum linear acceleration of the bioinspired backstepping has been greatly reduced, the demanding acceleration at initial stage reaches $9.47m/s^2$ for conventional backstepping control, whereas bioinspired backstepping control has $4.26m/s^2$ at its maximum. The lower acceleration that is needed based on bioinspired backstepping control for mobile robot implies the demanding torque from the motor is lower and therefore more practical than conventional backstepping control.

Although Figure 9(d) shows that both tracking methods are able to track a circular path, the conventional backstepping control has speed overshoot issues, which can be observed from Figure 9(e). The reason why this happens is caused by the design of conventional backstepping control from (39), the $C_1 e_D$ term shows that if there is an error occurring in the driving direction, the speed jump cannot be avoided. Therefore, the implementation of bioinspired model has overcome this speed jump issue and made the proposed tracking control even more practical for a mobile robot.

Figure 9(c) and 9(f) further demonstrates that if a larger tracking error occurs, the conventional backstepping control becomes impractical as the peak velocity reaches an uncontrollable value, especially for autonomous robots working under hard conditions, yet the bioinspired backstepping control constrains the peak velocity and makes it remains in a lower value.

V. CONCLUSION

In this paper, a novel tracking control of enhanced bioinspired backstepping controller, which contains the bioinspired backstepping controller and the torque controller, has been proposed. The proposed method is able to track the desired trajectory more accurately by considering both kinematics and dynamics of the mobile robot. Multiple studies in this paper supports that the proposed control strategy is able to provide the smooth velocity commands and reduce the effects of the noises. In addition, the KF and UKF are respectively integrated with the torque controller and bioinspired backstepping controller to provide better performance in state estimates for real-world applications. Furthermore, the entire closed-loop system is asymptotically stable and is guaranteed by Lyapunov stability theory. Overall, this paper presented a practical solution for a mobile robot tracking the desired trajectory under hard conditions with the presence of the system and measurement noises.

REFERENCES

[1] L. H. Juang and J. S. Zhang, "Visual tracking control of humanoid robot," *IEEE Access*, vol. 7, pp. 29 213–29 222, 2019.

[2] L. Ovalle, H. Ríos, M. Llama, V. Santibáñez, and A. Dzul, "Omnidirectional mobile robot robust tracking: Sliding-mode output-based control approaches," *Control Engineering Practice*, vol. 85, no. November 2018, pp. 50–58, 2019. [Online]. Available: https://doi.org/10.1016/j.conengprac.2019.01.002

[3] R. Wang, Q. Sun, D. Ma, and X. Hu, "Line Impedance Cooperative Stability Region Identification Method for Grid-tied Inverters Under Weak Grids," *IEEE Transactions on Smart Grid*, 2020. [Online]. Available: doi: 10.1109/tsg.2020.2970174

[4] R. Wang, Q. Sun, D. Ma, and Z. Liu, "The Small-Signal Stability Analysis of the Droop-Controlled Converter in Electromagnetic Timescale," *IEEE Transactions on Sustainable Energy*, vol. 10, no. 3, pp. 1459–1469, 2019.

[5] R. Wang, Q. Sun, P. Zhang, Y. Gui, D. Qin, and P. Wang, "Reduced-Order Transfer Function Model of the Droop-Controlled Inverter via Jordan Continued-Fraction Expansion," *IEEE Transactions on Energy Conversion*, 2020. [Online]. Available: doi: 10.1109/TEC.2020.2980033

[6] D. Chwa, "Tracking Control of Differential-Drive Wheeled Mobile Robots Using a Backstepping-Like Feedback Linearization," *IEEE Transactions on Systems, Man, and Cybernetics - Part A: Systems and Humans*, vol. 40, no. 6, pp. 1285–1295, 2010.

[7] D.-H. Kim and J.-H. Oh, "Tracking control of a two-wheeled mobile robot using input-output linearization," *Control Engineering Practice*, vol. 7, no. 3, pp. 369–373, 1999.

[8] C. Aguilar-Avelar and J. Moreno-Valenzuela, "New feedback linearization-based control for arm trajectory tracking of the furuta pendulum," *IEEE/ASME Transactions on Mechatronics*, vol. 21, no. 2, pp. 638–648, 2016.

[9] B. Sun, D. Zhu, F. Ding, and S. X. Yang, "A novel tracking control approach for unmanned underwater vehicles based on bio-inspired neurodynamics," *Journal of Marine Science and Technology (Japan)*, vol. 18, no. 1, pp. 63–74, 2013.

[10] Z. Chu, D. Zhu, S. X. Yang, and G. E. Jan, "Adaptive Sliding Mode Control for Depth Trajectory Tracking of Remotely Operated Vehicle with Thruster Nonlinearity," *The Journal of Navigation*, vol. 70, no. 1, pp. 149–164, 2020.

[11] X. Yang, P. Wei, Y. Zhang, X. Liu, and L. Yang, "Disturbance Observer Based on Biologically Inspired Integral Sliding Mode Control for Trajectory Tracking of Mobile Robots," *IEEE Access*, vol. 7, pp. 48 382–48 391, 2019.

[12] B. Sun, D. Zhu, and S. X. Yang, "A Bioinspired Filtered Backstepping Tracking Control of 7000-m Manned Submarine Vehicle," *IEEE Transactions on Industrial Electronics*, vol. 61, no. 7, pp. 3682–3693, 2014.

[13] C.-Z. Pan, X.-Z. Lai, S. X. Yang, and M. Wu, "Backstepping Neurodynamics based Position-Tracking Control of Underactuated Autonomous Surface Vehicles," in *2013 25th Chinese Control and Decision Conference (CCDC)*. IEEE, 2013, pp. 2845–2850.

[14] S. X. Yang, A. Zhu, G. Yuan, and M. Q. Meng, "A Bioinspired Neurodynamics-Based Approach to Tracking Control of Mobile Robots," *IEEE Transactions on Industrial Electronics*, vol. 59, no. 8, pp. 3211–3220, 2012.

[15] M. Cui, "Observer-Based Adaptive Tracking Control of Wheeled Mobile Robots with Unknown Slipping Parameters," *IEEE Access*, vol. 7, pp. 169 646–169 655, 2019.

[16] J. Chi, H. Yu, and J. Yu, "Hybrid Tracking Control of 2-DOF SCARA Robot via Port-Controlled Hamiltonian and Backstepping," *IEEE Access*, vol. 6, pp. 17 354–17 360, 2018.

[17] C.-Z. Pan, X.-Z. Lai, S. X. Yang, and M. Wu, "Expert Systems with Applications An efficient neural network approach to tracking control of an autonomous surface vehicle with unknown dynamics," *Expert Systems With Applications*, vol. 40, no. 5, pp. 1629–1635, 2013. [Online]. Available: http://dx.doi.org/10.1016/j.eswa.2012.09.008

[18] Z. Chu, D. Zhu, and S. X. Yang, "Observer-Based Adaptive Neural Network Trajectory Tracking Control for Remotely Operated Vehicle," *IEEE Transactions on Neural Networks and Learning Systems*, vol. 28, no. 7, pp. 1633–1645, 2017.

[19] S. H. Lee, W. D. Jang, and C. S. Kim, "Tracking-by-segmentation using superpixel-wise neural network," *IEEE Access*, vol. 6, pp. 54 982–54 993, 2018.

[20] S. A. Gadsden and S. R. Habibi, "A New Robust Filtering Strategy for Linear Systems," *Journal of Dynamic System, Measurement, and Control*, vol. 135, no. 1, p. 014503, 2013.

[21] M. Attari, S. Habibi, and S. A. Gadsden, "Target Tracking Formulation of the SVSF With Data Association Techniques," *IEEE Transactions on Aerospace and Electronic Systems*, vol. 53, no. 1, pp. 12–25, 2017.

[22] S. A. Gadsden, S. R. Habibi, and T. Kirubarajan, "Kalman and Smooth Variable Structure Filters for Robust Estimation," *IEEE Transactions on Aerospace and Electronic Systems*, vol. 50, no. 2, pp. 1038–1050, 2014.

[23] A. Gadsden, H. Saeid, and D. Dunne, "Nonlinear Estimation Techniques Applied on Target Tracking Problems," *journal of Dynamic Systems, Measurement, and Control*, vol. 134, no. 5, p. 5450(13), 2012.

[24] A. Vaccarella, E. D. Momi, A. Enquobahrie, and G. Ferrigno, "Unscented Kalman Filter Based Sensor Fusion for Robust Optical and Electromagnetic Tracking in Surgical Navigation," *IEEE TRANSACTIONS ON INSTRUMENTATION AND MEASUREMENT*, vol. 62, no. 7, pp. 2067–2081, 2013.

[25] R. Fierro and F. L. Lewis, "Control of a Nonholonomic Mobile Robot : Backstepping Kinematics into Dynamics," in *Proceedings of the 34th Conference on Decision & Control*, New Orleans, 1995, pp. 3805–3810.

[26] S. X. Yang and M. Meng, "An efficient neural network approach to dynamic robot motion planning," *Neural Networks*, vol. 13, no. 2, pp. 143–148, 2000.

[27] B. Rui, Y. Yang, and W. Wei, "Nonlinear Backstepping Tracking Control for a Vehicular Electronic Throttle with Input Saturation and External Disturbance," *IEEE Access*, vol. 6, pp. 10 878–10 885, 2017.

[28] J. Zhou, X. Zhao, T. Chen, Z. Yan, and Z. Yang, "Trajectory Tracking Control of an Underactuated AUV Based on Backstepping Sliding Mode with State Prediction," *IEEE Access*, vol. 7, pp. 181 983–181 993, 2019.

[29] Z. Yan, Z. Yang, J. Zhang, J. Zhou, A. Jiang, and X. Du, "Trajectory tracking control of uuv based on backstepping sliding mode with fuzzy switching gain in diving plane," *IEEE Access*, vol. 7, pp. 166 788–166 795, 2019.

[30] E. A. Wan and R. v. d. Merwe, "Unscented Kalman filter for nonlinear estimation," in *IEEE 2000 Adaptive Systems for Signal Processing, Communications, and Control Symposium (Cat. No.00EX373)*, 2000, pp. 153–158.

[31] L. D'Alfonso, W. Lucia, P. Muraca, and P. Pugliese, "Mobile robot localization via EKF and UKF: A comparison based on real data," *Robotics and Autonomous Systems*, vol. 74, pp. 122–127, 2015. [Online]. Available: http://dx.doi.org/10.1016/j.robot.2015.07.007

[32] J. Zarei and A. Ramezani, "Performance Improvement for Mobile Robot Position Determination Using Cubature Kalman Filter," *Journal of Navigation*, vol. 71, no. 2, pp. 389–402, 2018.

ZHE XU received B.ENG. degree in Mechanical Engineering in 2018 and M.A.Sc. degree in Engineering Systems and Computing in 2019 from the University of Guelph. He is currently pursuing the Ph.D. degree in Engineering Systems and Computing with the School of Engineering at the University of Guelph under Professor Simon X. Yang's Supervision. His research interests include tracking control, estimation theory, robotics, and intelligent systems.

SIMON X. YANG (S'97–M'99–SM'08) received the B.Sc. degree in engineering physics from Beijing University, Beijing, China, in 1987, the first of two M.Sc. degrees in biophysics from the Chinese Academy of Sciences, Beijing, in 1990, the second M.Sc. degree in electrical engineering from the University of Houston, Houston, TX, in 1996, and the Ph.D. degree in electrical and computer engineering from the University of Alberta, Edmonton, AB, Canada, in 1999. Dr. Yang is currently a Professor and the Head of the Advanced Robotics and Intelligent Systems Laboratory at the University of Guelph, Guelph, ON, Canada. His research interests include robotics, intelligent systems, sensors and multi-sensor fusion, wireless sensor networks, control systems, machine learning, fuzzy systems, and computational neuroscience.

Prof. Yang he has been very active in professional activities. He serves as the Editor-in-Chief of International Journal of Robotics and Automation, and an Associate Editor of IEEE Transactions on Cybernetics, IEEE Transactions of Artificial Intelligence, and several other journals. He has involved in the organization of many international conferences.

STEPHEN ANDREW GADSDEN (M'09–SM'19) received the Ph.D. degree in state and parameter estimation theory from McMaster University, Hamilton, ON, Canada, in 2011.

He was an Assistant Professor with the Department of Mechanical Engineering, University of Maryland, Baltimore, MD, USA, from 2014 to 2016. He is currently an Associate Professor with the College of Engineering and Physical Sciences, University of Guelph, Guelph, ON, Canada. His work involves the optimal realization and further advancement of robust filtering strategies with applications in mechatronics and aerospace technology. He has a broad research background that includes the consideration of state and parameter estimation strategies, variable structure theory, fault detection and diagnosis, mechatronics, target tracking, cognitive systems, and artificial intelligence.

He is an elected Fellow of ASME, and a Professional Engineer of Ontario. He is a 2019 SPIE Rising Researcher award winner based on his work in intelligent estimation theory and is also a 2018 Ontario Early Researcher (ERA) award winner based on his work in intelligent condition monitoring strategies.